AGGREGATE SIMULATION MODELING OF AN MRI DEPARTMENT USING EFFECTIVE PROCESS TIMES

F.J.A. Jansen
L.F.P. Etman
J.E. Rooda
I.J.B.F. Adan

Department of Mechanical Engineering
Eindhoven University of Technology
PO Box 513, 5600 MB Eindhoven, THE NETHERLANDS

ABSTRACT

Magnetic Resonance Imaging (MRI) requires expensive diagnostic equipment and is labor intensive. To evaluate the effective use of the MRI resources a curve of flow time versus throughput may be helpful in quantifying the trade-off between patient waiting time and resource utilization, and in providing insight into operational time losses and variability. This curve may be obtained by simulation. However, building a detailed simulation model of an MRI department requires expertise typically unavailable in hospitals. To overcome this difficulty, we seek for an appropriate aggregate model of the MRI department, either a simulation or an analytical model. The aggregate model parameters are to be determined from hospital patient arrival and departure times. We study three different aggregate models for use in the MRI setting. To be able to evaluate the prediction accuracy of the candidate aggregate models we use a detailed simulation model as virtual MRI department.

1 INTRODUCTION

Magnetic Resonance Imaging (MRI) is used in many hospitals for the diagnosis of a variety of illnesses. MRI requires rather expensive diagnostic equipment, and is quite labor intensive. Before the MRI scan, the patient needs to be prepared and the MRI scanner needs to be setup. During the scan, the scan operation is monitored from the control room. After the scan, the patient is escorted back to the change room.

Given the cost of equipment and the labor intensive operation, the hospital strives to maximize the number of patients that can be scanned during a working day. To reduce idle time of the MRI scanner, preparation of a patient is usually done while another patient is being scanned. Furthermore, patients are asked to arrive at designated appointment slots, well in advance of their actual treatment since the times needed for preparation, setup and scanning are subject to variability. Also unscheduled emergency scans contribute to this variability.

There is a remarkable similarity between MRI scanning in hospitals and lithography scanning in semiconductor manufacturing: the operation is expensive and organized as a sequence of process steps. Performance analysis approaches used in semiconductor manufacturing may therefore be helpful in the MRI hospital setting. For instance, in semiconductor manufacturing, the flow time-throughput characteristic curve of a workstation is commonly employed to quantify the trade-off between throughput and flow time (Schoemig 1999). A similar trade-off is present in the hospital: the conflict between patient waiting time and utilization of resources (scanners, doctors, technicians), (Fomumdam and Herrmann 2007).

The flow time-throughput curve may be obtained from simple analytical queuing equations, such as Sakasegawas and Whitts closed form $G/G/m$ expression, see for instance the book by Hopp and Spearman (2008). A complication is the flow of process steps in the MRI system which makes the $G/G/m$ representation

less accurate. Alternatively, the flow time-throughput curve may be obtained using a simulation model that includes all relevant shop floor details (Park et al. 2002). However, building a detailed simulation model is quite elaborate and requires the collection of the necessary input data regarding the modeled details.

At the 2011 WSC conference we have presented an overview of our research efforts to develop *aggregate* models for queuing performance analysis of semiconductor equipment (Etman et al. 2011). The various details are not modeled in detail, but their contribution is lumped into an *effective process time* (EPT) distribution. The EPT distribution parameters are estimated directly from arrival and departure data collected from the manufacturing system in operation. While the aggregate model is trained by data obtained at a single utilization (throughput) level, the aggregate model can be used to predict the flow time performance at other utilization levels as well. Thus, a flow time-throughput curve is obtained.

We investigate the suitability of EPT-based aggregate modeling for operational health care modeling (Brailsford 2007), the MRI department in particular. We rely on a detailed simulation model as virtual MRI department to study the question: How accurate are the EPT-based aggregate models we have developed so far, or do we need a new class of aggregate models for the health care application? Through the simulated MRI environment, we can evaluate the prediction accuracy of candidate aggregate models at utilization levels other than the throughput training level, which is not possible if we use actual patient arrival and departure data from the hospital only. The detailed MRI simulation model we use in this paper was built for a hospital in the Netherlands in a related project (Pagoria 2011). The detailed model was validated using measurements from the hospital floor and was shown to provide a reasonable accurate representation of the MRI department under investigation.

The outline of the paper is as follows. We first present in Section 2 the detailed simulation model which serves as our virtual MRI department. In the subsequent sections we study three aggregate models. The first two are existing models, see Etman et al. (2011). The third one is new. In Section 3 we start with the 'classical' $G/G/1$ model and determine the mean and variance of the effective process time from arrival and departure times obtained from the virtual MRI department. The accuracy of this model for the (virtual) MRI department is shown to be rather poor, so we consider in Section 4 an existing work-in-progress-dependent $G/G/1$ type of aggregate model. This yields a significant improvement. But we also notice that the wip-dependency is limited to just a few wip levels. Therefore, in Section 5 we finally investigate a novel waiting time dependent aggregate model that is more suited for the MRI case.

2 DETAILED SIMULATION MODEL: VIRTUAL MRI DEPARTMENT

In the detailed simulation model the flow of patients through a single MRI scanner is modeled. The model is visualized in Figure 1, and briefly explained below. The following processes are identified:

G Generator, generates new patients according to a deterministic inter-arrival scheme (scheduled appointments) and a uniform distribution to indicate the patient type (43% with and 57% without contrast preparation).

W_i Patient waiting area. All patients that enter W_1 are redirected to W_2 except for 55% of the patients that require preparation.

R_i Relocation of a patient under guidance of a technician (nurse specialized for the activities in the MRI department). The relocation time is a sample from a triangular distribution with min, mean, max = 0.45, 0.50, 0.55 [min].

P Preparation room. The technician prepares the intravenous injection device in the patients arm, necessary for the contrast liquid injection during the scan. The preparation time is modeled by a triangular distribution with min, mean, max = 3.0, 4.0, 5.0 [min].

C^2 Two change rooms (for patients to undress or dress). The time to (un)dress is modeled as Gamma distributed with shape parameter 3.41 and scale parameter 0.86. The same parameter values are used for time to undress and time to dress.
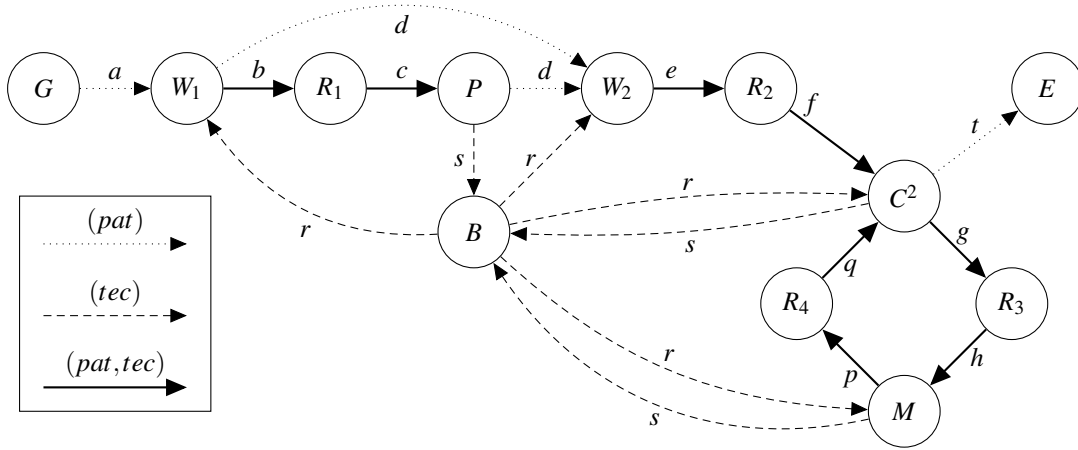
Figure 1: Detailed simulation model of the MRI department (single scanner). Circles indicate processes, arrows indicate communication channels.

- *M*   MRI room. The activities include setup of the patient on the MRI table and setup of the MRI scanner (Gamma distributed time to setup, with shape parameter 2.08 and scale parameter 2.01), the MRI scanning (Gamma distribution with shape parameter 7.86 and scale parameter 2.67), and the after-scan activities (Gamma distribution with shape parameter 1.66 and scale parameter 1.81). If a patient requires preparation but was not prepared in the preparation room *P*, then preparation is executed in the MRI room during step *M*, which takes a deterministic 6.00 [min].
- *B*   Technician buffer, contains technicians waiting for a new work cycle assignment. There is a fixed number of technicians. Technicians are either assigned to a work cycle or waiting in *B*.
- *E*   Exit. The patient flow time is calculated here.

There are four types of work cycles a technician can be assigned to:

1. Guide (relocate) a patient from waiting area W_1 to preparation room *P*, and prepare for contrast liquid injection.
2. Guide a patient from waiting area W_2 to change room *C*.
3. Guide a patient from change room *C* to MRI room *M*, do the MRI setup, the MRI scan, the after scan activities, and guide the patient back to change room *C*.
4. Assist another technician with MRI setup (part of *M*), which requires two technicians.

A work cycle can only start once the receiving process is vacant. The flow of patients (pat), technicians (tec), and patients accompanied by technicians (pat,tec) is visualized in Figure 1.

3   *G/G/*1 AGGREGATE MODEL

Our first experiment is to aggregate the MRI detailed model into a simple *G/G/*1 representation with the mean and coefficient of variation of the *effective process time* (EPT) determined from arrivals (generator *G*) and departures (exit *E*) measured in the detailed model. For each departing patient its effective process time is calculated using:

$$e_i = d_i - \max(a_i, d_{i-1}) \tag{1}$$

where e_i is the EPT realization due to the i-th patient departing from the MRI department, d_i is the departure time of the i-th departing patient, a_i is the arrival time of the i-th departing patient, and d_{i-1} is the departure time of the $(i-1)$-th departing patient.

We simulated one million patients (excluding a warm-up period of fifty thousand patients) for a range of inter-arrival rates. We calculated mean effective process time t_e [min], squared coefficient of variation c_e^2, and associated 90% confidence intervals using the batch means method. See Table 1.

Table 1: Mean effective process time t_e [min] and squared coefficient of variation of the effective process time c_e^2 for various arrival rates. t_a denotes the mean inter arrival time [min], δ/δ_{max} the fraction of throughput and maximum throughput, and CI the two-sided 90% confidence interval.

		MRI model	
t_a	$\delta/\delta_{\mathbf{max}}$	$t_{\mathbf{e}} \pm$ (CI/2)	$c_{\mathbf{e}}^2 \pm$ (CI/2)
0.0001	1.00	29.82 ± 0.1117	0.090 ± 0.00019
30	0.99	29.99 ± 0.0077	0.090 ± 0.00019
32	0.93	31.50 ± 0.0049	0.092 ± 0.00020
34	0.88	32.80 ± 0.0061	0.089 ± 0.00021
36	0.83	33.88 ± 0.0075	0.085 ± 0.00019
38	0.78	34.77 ± 0.0088	0.081 ± 0.00019
40	0.75	35.49 ± 0.0104	0.077 ± 0.00021
50	0.60	37.29 ± 0.0141	0.065 ± 0.00017
60	0.50	37.69 ± 0.0156	0.062 ± 0.00017
80	0.37	37.76 ± 0.0155	0.061 ± 0.00015

Table 1 shows that t_e and c_e depend on the inter-arrival rate. For $t_a = 80$ [min], t_e equals the mean flow time of a patient in an empty system (37.76 [min]), whereas for $t_a = 30$ [min], t_e is approximately equal to the inter-arrival time, i.e. the inverse of the throughput of the system. This means the MRI department cannot really be modeled as a $G/G/1$ system, unless the system operates at a very high throughput. This is confirmed by Figure 2.

The blue, the green, and the red lines in Figure 2 correspond to flow time-throughput predictions by the $G/G/1$ aggregation with the t_e and c_e^2 set to the values in Table 1 corresponding to $t_a = 50, 38, 32$, respectively. We refer to these t_a values as the throughput training points of the aggregate model. The solid lines correspond to the prediction obtained using analytical $G/G/1$ queuing approximation (Hopp and Spearman 2008):

$$\varphi = \frac{c_a^2 + c_e^2}{2} \frac{u}{1-u} t_e + t_e \tag{2}$$

with $u = t_e/t_a$, and $c_a^2 = 0$ for the deterministic arrivals. The lines connecting data points depicted by '+' signs in red, green en blue, were obtained by simulating the $G/G/1$ aggregate model for various arrival rates. In the picture, the center '+' represents the simulated mean, the upper '+' the upper bound of the 90% confidence interval on the mean, and the bottom '+' the confidence lower bound. Only for high throughput levels the three crosses can be identified; for the other levels they lie approximately on top of each other. Due to the deterministic arrivals, (2) is an approximation and slightly deviates from the simulated response in particular for lower throughput levels.

With black, the simulated responses of the *detailed* simulation model are depicted. Clearly, the vertical asymptote predicted by the $G/G/1$ models is located at a too low throughput; the higher the throughput training point, the better the prediction. Also, the predicted horizontal asymptote is subject to some error; this error gets smaller for a lower throughput training point. Obviously this is due to the dependency of t_e on the arrival rate, as observed in Table 1.

4 WIP-DEPENDENT *G/G/1*-TYPE OF AGGREGATE MODEL

In Etman et al. (2011), a second class of EPT-based aggregate models is described: aggregate models that depend on the work-in-progress (wip). The idea is to make the EPT distribution in the aggregate model
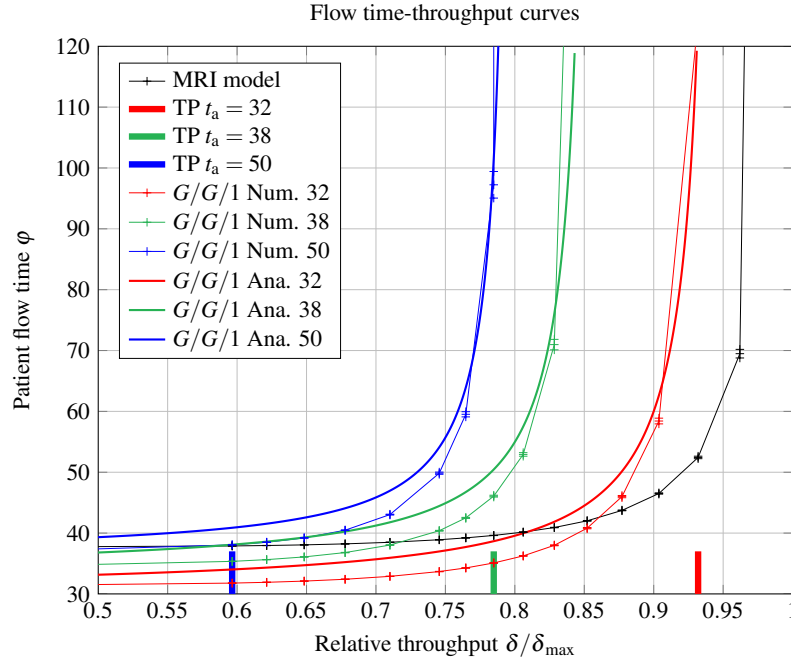
Flow time-throughput curves

Figure 2: Flow time-throughput curves predicted by the *G/G*/1 aggregate model (analytical and simulation) for three throughput training points (TPs) and the true curve calculated by the detailed simulation model.

wip dependent, and to measure this wip dependency from the stochastic wip fluctuations in the operating system to be aggregated. For the MRI department this means that we register for each patient besides the effective process time, also the wip the patient experiences during its visit. Then we can sort the EPT realizations in accordance with the wip-level, which provides us with a wip-dependent EPT distribution that we can use to build a wip-dependent *G/G*/1 alike aggregate (simulation) model.

Veeger et al. (2010) developed such wip-dependent aggregate models for semiconductor equipment. They noticed that EPTs started upon arrival (for lots entering an empty system), behave differently from the other EPTs started upon departure (thus for lots that have been waiting in the queue). This is also true for a wip-dependent *G/G*/1 type of aggregation of the MRI department. The EPT of a patient entering an empty MRI department will always be the sum of the processing times of the various steps in the MRI department (assuming that no overtaking occurs), which is independent of the arrival rate. On the other hand, the EPTs that start upon departure of a previous patient, do depend on the arrival rate. The EPT becomes shorter the more crowded it gets in the MRI department.

This means that upon departure of a patient we register the EPT, the wip upon EPT start, and the event responsible for the EPT start (start upon arrival or start upon departure). These three data objects can be calculated from the registered arrival and departure times. We distinguish two EPT distributions: one for EPTs started upon arrival, and one for EPTs started upon departure. The first distribution is wip independent. The second distribution is wip dependent, for instance the mean effective process time is expected to decrease for increasing number of patients in the system (i.e. for increasing arrival rate).

In the wip-dependent aggregate simulation model we use multiple process time distributions: one for each wip-level with the mean and variance obtained from the measured EPT distributions. A fictitious wip-level 'zero' is introduced corresponding to the distribution of EPTs that started upon arrival. Also, a certain maximum wip level N is identified where the system operates near its maximum throughput and has as such become workload independent.

For a range of arrival rates, we did several simulation runs of one million patients (excluding warm-up period). The number of EPTs observed for each wip level are presented in Table 2. Figure 3 depicts the measured mean EPT values $t_e(w)$ as a function of the wip. For c_e^2 a similar picture can be made.

Table 2: Distribution of 1 million EPT realizations over WIP levels for different deterministic inter-arrival times in actual numbers.

# EPTs	WIP Level							
t_a	0	1	2	3	4	5	6	≥ 7
30	3926	51869	56052	52689	48645	46059	43309	697451
32	114799	667139	176170	34168	6552	968	191	13
34	236998	710707	50054	2192	48	1		-
36	360490	627164	12244	99	3	-	-	-
38	476636	520368	2989	6	1	-	-	-
40	581369	417850	780	1	-	-	-	-
45	779000	220959	41	-	-	-	-	-
50	895841	104158	1	-	-	-	-	-
60	982714	17286	-	-	-	-	-	-
80	999788	212	-	-	-	-	-	-

From Table 2 and Figure 3 we observe the following:

1. Figure 3 confirms that for patients entering an empty system (wip level zero), the t_e is independent of the throughput training level, equal to the mean flow time in an empty system (no queuing).
2. Figure 3 shows a monotonically decreasing $t_e(w)$.
3. Figure 3 shows that the wip dependence is limited to wip levels 0, 1 and 2; for higher wip levels a t_e asymptote is reached which relates to the maximum throughput of the MRI department.
4. Table 2 shows that for low arrival rates, the number of patients in the MRI department is mostly one (wip levels zero and one). Only for arrival rates approaching the maximum throughput of the system, higher wip-levels are observed.
5. For wip level one, Figure 3 shows that t_e depends on the throughput training level (arrival rate).
6. Finally, Figure 3 seems to suggest that the measured t_e can get below the theoretical minimum t_e one would expect at first sight, being the reciprocal of the maximum throughput.

From these observations we draw the following conclusions:

-   Observation 1 confirms that, similar to Veeger et al. (2010), in the aggregate model we need to distinguish between effective process times that start upon arrival of a patient entering an empty system, and process times that start upon departure of a previous patient.
-   Observation 2 means that the prediction accuracy of the aggregate model is expected to improve if we account for the work load dependency. This was also the very reason in our previous work to develop wip-dependent aggregate models, see Etman et al. (2011).
-   Observation 3 is new to us. That is, in our semiconductor applications the monotonic decrease typically occurred on a wider range of wip levels. The reason is twofold: (a) in the semiconductor applications we typically aggregated multi-machine workstations into a single-server wip-dependent aggregate model, (b) the variability present in the semiconductor applications seems to be much higher than in the MRI department. Note that the c_e^2 values reported in Table 1 are rather low.
-   Observation 4 stresses that for certain throughput training levels certain wip levels may not contain sufficient EPT realizations to compute an accurate mean value. To properly train the aggregate
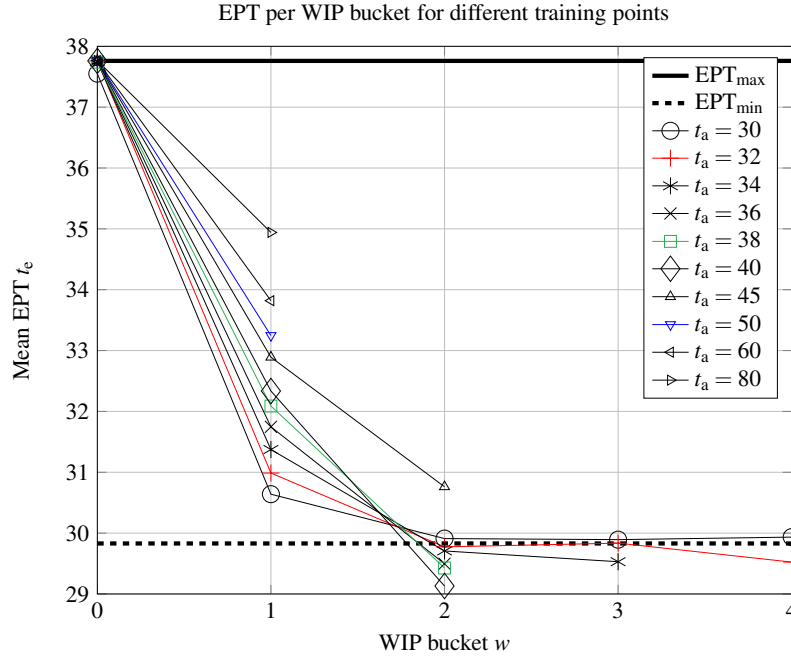
EPT per WIP bucket for different training points

Figure 3: Measured mean EPT per WIP level for different inter-arrival times. EPT_{max} and EPT_{min} denote the analytically determined maximum and minimum EPT.

            model we need to account for certain wip levels that may have insufficient EPT realizations to calculate a reliable t_e and c_e^2 value. A similar observation was made by Veeger et al. (2010).
- Observation 5 is again new to us, at least to some extend. From our earlier work we already knew that the wip-dependent behavior typically cannot be fully estimated from monitoring the stochastic behavior of the system at a *single* utilization level (throughput training point). Nevertheless we have always found it remarkable how much we can actually reconstruct. Figure 3 suggests a rather significant dependency of $t_e(w = 1)$ on the throughput training point, which may negatively affect the prediction accuracy of the aggregate model. The actual prediction accuracy can only be investigated by implementing the aggregate model and comparing its response with the detailed simulation model, which will be presented shortly.
- Finally, Observation 6 is remarkable indeed, and was noticed earlier by Veeger et al. (2011).
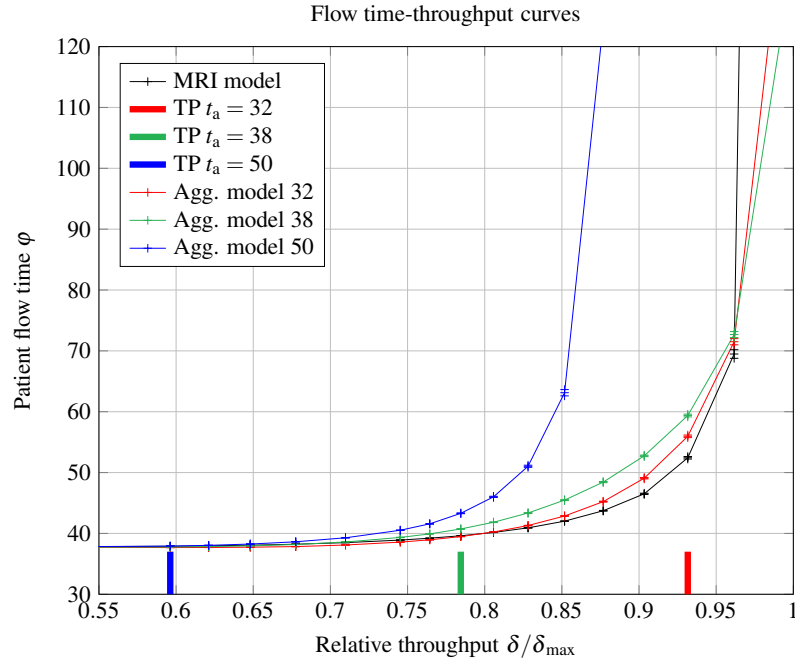
            We built a wip-dependent $G/G/1$ type of aggregate model (simulation model) for training levels: $t_a = 32$, 38, and 50 [min], using five, three, and two wip-levels for EPT distributions, respectively (motivated by the number of EPT realizations given in Table 2). For each wip level the effective process time distribution is represented by a Gamma distribution with the parameters given in Table 3.

            The flow time-throughput curves (red, green, and blue) predicted by the aggregate model are depicted in Figure 4. The black curve is the true response by the detailed model. Compared to Figure 2 this is a clear improvement, in particular for training levels $t_a = 32$ and $t_a = 38$. For $t_a = 50$, some of the wip-dependent behavior is not covered due to the missing second wip level for the EPT distribution, which causes a severe error in the estimate of the location of the vertical asymptote. Note that the horizontal asymptote is correctly estimated for all training points due to the training point independence in wip level 0.

            Inclusion of the wip-dependent behavior in the aggregate model yields a significant improvement compared to the classical $G/G/1$ aggregation. The location of the predicted vertical asymptote is slightly to the right of the true asymptote, which is due to Observation 6. Figure 4 also provides for a new observation: for training points $t_a = 32$ and $t_a = 38$ we observe an overestimation of the flow time at the training point.

Table 3: Gamma shape and scale parameters for the gamma distributions fitted to the EPT data per training point per WIP level w.

	Measurement		Gamma parameters		t_e	c_e^2
Training Point	w	n	shape a	scale b	$(a \cdot b)$	$(1/a)$
	0	114799	16.3454	2.3100	37.7579	0.06118
	1	667139	10.8098	2.8666	30.9874	0.09251
$t_a = 32$	2	176170	10.6392	2.7985	29.7738	0.09400
	3	34168	10.5879	2.8177	29.8334	0.09445
	4	7724	10.7677	2.7419	29.5240	0.09287
	0	476636	16.4436	2.2951	37.7397	0.06081
$t_a = 38$	1	520368	10.8617	2.9543	32.0887	0.09207
	2	2996	9.8773	2.9792	29.4265	0.10124
$t_a = 50$	0	895841	16.3684	2.3073	37.7668	0.06109
	1	104159	11.3120	2.9391	33.2471	0.08840

Figure 4: Flow time-throughput curves predicted by the wip-dependent $G/G/1$-type aggregate model for three throughput training points (TPs) and the true curve calculated by the detailed simulation model.

This is noteworthy, since in our earlier work the aggregate model predictions are usually quite accurate near the training point (see e.g. Figure 3 (b) in Etman et al. (2011)). We conjecture this can be attributed to the workload dependency within the wip levels of the EPT distributions, level one in particular.

5   WAITING TIME DEPENDENT *G/G/*1-TYPE OF AGGREGATE MODEL

Motivated by the observation that the wip dependency is limited to just a few wip levels (resulting in workload dependency within wip levels of the EPT distributions) we explore a novel type of aggregate

model: a waiting time dependent *G/G/*1 type of aggregate model. The idea is to let t_e and c_e^2 depend on the *waiting time* (instead of the wip) a patient has experienced upon its process time start in the aggregate model. From the arrival and departure data, this waiting time can be calculated as follows:

$$q_i = \max(0, d_{i-1} - a_i) \tag{3}$$

The effective process time is again computed from (1). We thus arrive at a cloud of points (e_i, q_i), and may use any suitable discretization in the continuous waiting time domain to obtain approximations for the relations $t_e(q)$ and $c_e^2(q)$. In this paper we have relied on calculating the moving average using a certain moving window size. An example is given in Figure 5. To the moving average we fit some exponential type of function to obtain explicit relations for $t_e(q)$ and $c_e^2(q)$ that can be used in the aggregate model.
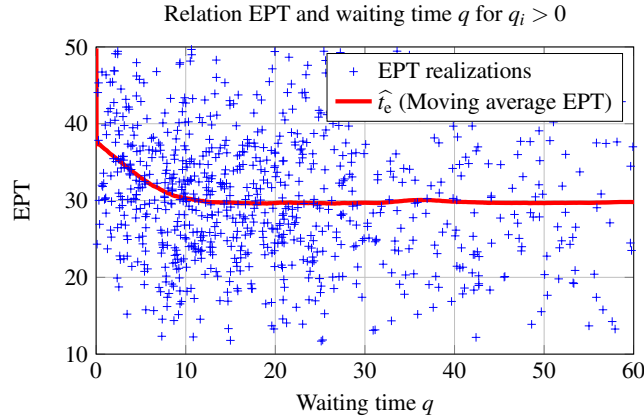

Figure 5: A cloud of points (e_i, q_i). The red curve is the moving average that is used as trend line to obtain relation $t_e(q)$.

The aggregate model consists of a patient arrival distribution (deterministic inter arrival times in our case), an infinite-capacity queue and a single server. The server uses two process time distributions: 1) a waiting time independent effective process time distribution for patients arriving in an empty system, 2) a waiting time dependent effective process time distribution, with the mean and variance given by $t_e(q)$ and $c_e^2(q)$ for patients who arrived in a non-empty system. Upon sampling a new service time for the next patient, the waiting time this patient has experienced until start of service determines the distribution parameter values. So for each patient of the second category the process time distribution parameters are (slightly) different. The aggregate model building procedure can be summarized as:

- Collect arrival and departure times at the system to be aggregated.
- Calculate for each departing patient an EPT realization e_i and waiting time realization q_i.
- From the (e_i, q_i) data obtain approximate (preferably explicit) expressions for $t_e(q)$ and $c_e^2(q)$; distinguish between EPTs started upon arrival ($q = 0$), and EPTs started upon departure of a previous patient ($q > 0$).
- Build the aggregate model using $t_e(q = 0)$ and $c_e^2(q = 0)$, respectively $t_e(q > 0)$ and $c_e^2(q > 0)$ as means and variances in the two process time distributions of the aggregate server.

The result of the first three steps are presented in Figures 6(a) and 6(b). The two graphs in Figure 6 present $t_e(q > 0)$ and $c_e^2(q > 0)$, both the observed moving average and the exponential fit, for arrival rates $t_a = 32, 38,$ and 50, respectively. For $q = 0$, we found $t_e = 37.76$ and $c_e^2 = 0.061$, irrespective of the training point. We observe:

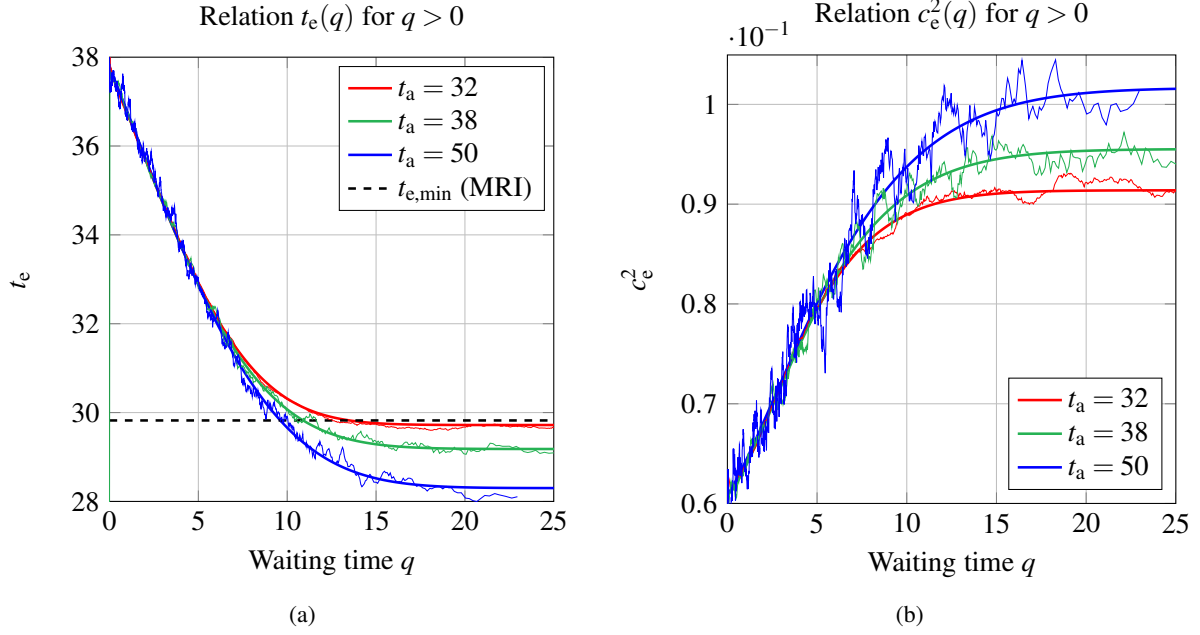- t_e is monotonically decreasing, whereas c_e^2 is monotonically increasing.

Figure 6: Moving averages and exponential function fits for $t_e(q)$ and $c_e^2(q)$ for the three training points.

- c_e^2 is very low (similar as in Table 1).
- The horizontal asymptote of $t_e(q)$ is below the minimum expected value (reciprocal of the maximum throughput). For $t_a = 50$ this difference is quite pronounced.
- The chosen exponential function is able to quite accurately fit the moving averaged data.
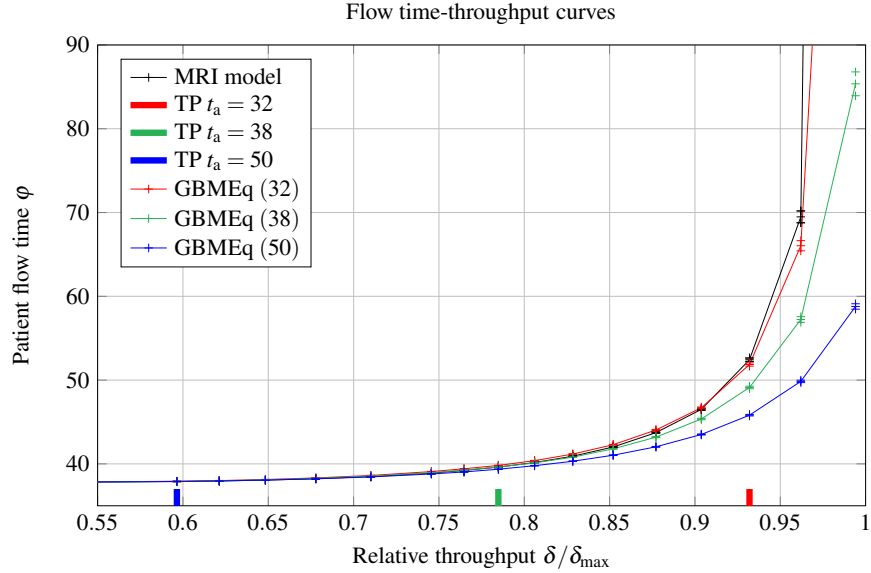

Figure 7: Flow time-throughput curves predicted by the waiting time-dependent $G/G/1$-type aggregate model - denoted GBMEq - for three throughput training points (TPs) and the true curve calculated by the detailed simulation model.

The flow time predictions by the aggregate model are presented in Figure 7. Note again that the horizontal asymptote is correctly estimated, and also the flow time prediction is accurate near the training throughput level, irrespective of the training point. We now consistently have a vertical asymptote estimated to the right of the true vertical asymptote. This is due to the underestimation of the t_e asymptote in Figure 6(a). Apparently for low throughput levels we have difficulties to reconstruct the true maximum throughput value from the observed (e_i, q_i) values. For higher training throughput the prediction becomes more accurate.

6 CONCLUSION

We have investigated three types of models for aggregate simulation modeling of an MRI department: 1) a *G*/*G*/1 model, 2) a wip-dependent *G*/*G*/1 type of model, and 3) a novel waiting-time dependent *G*/*G*/1 type of model. To investigate the accuracy of the aggregate models, a detailed simulation model of an MRI department of a hospital in the Netherlands has been used. The process time distribution parameters of the aggregate models are estimated from arrival and departure times generated by the detailed MRI simulation model. Subsequently the flow-time throughput curves predicted by the aggregate models have been compared with the 'true' curve generated by the detailed MRI simulation model.

The accuracy of the 'classical' *G*/*G*/1 model is inferior to the wip-dependent and the waiting-time dependent model. The effective process time model parameters are workload dependent, which can be better captured by the latter two aggregate model variants. A particular property of the studied MRI system is that the workload dependency is limited to just a few wip levels. Maximum throughput is reached once two or more patients are in the system. The proposed waiting-time dependent aggregate model provides a more accurate flow-time prediction than the wip-dependent aggregate model. The waiting-time dependent model avoids discretization errors, but still estimates a too high maximum throughput due to the underestimation of the t_e asymptote. We note however that the maximum throughput estimation becomes more accurate as the training throughput approaches the true maximum throughput. In practice many MRI departments operate at a rather high utilization.

On the basis of our simulation study, we conclude that the new waiting time dependent model is a promising candidate for EPT-based performance modeling of an MRI department. The next step is to study the aggregate model building from the hospital data perspective, for instance regarding the typically limited number of patient arrival and departure events and the strong daily fluctuations in health care systems.

REFERENCES

Brailsford, S. C. 2007, December. "Tutorial: Advances and challenges in healthcare simulation modeling". In *Proceedings of the 2007 Winter Simulation Conference*, edited by S. G. Henderson, B. Biller, M.-H. Hsieh, J. Shortle, J. D. Tew, and R. R. Barton, 1436–1448. Piscataway, New Jersey: Institute of Electrical and Electronics Engineers, Inc.

Etman, L. F. P., C. P. L. Veeger, E. Lefeber, I. J. B. F. Adan, and J. E. Rooda. 2011, December. "Aggregate Modeling of Semiconductor Equipment using Effective Process Times". In *Proceedings of the 2011 Winter Simulation Conference*, edited by S. Jain, R. R. Creasey, J. Himmelspach, K. P. White, and M. Fu, 1795–1807. Piscataway, New Jersey: Institute of Electrical and Electronics Engineers, Inc.

Fomumdam, S., and J. W. Herrmann. 2007. "A Survey of Queueing Theory Applications in Healthcare". Technical Report TR2007-24, Institute for Systems Research, University of Maryland. Available via http://hdl.handle.net/1903/7222.

Hopp, W. J., and M. L. Spearman. 2008. *Factory Physics: Foundations of Manufacturing Management*. 3rd ed. New York: IRWIN/McGraw-Hill.

Pagoria, G. 2011. "Analysis and Performance Improvement of MRI Departments". Technical Report Technical report SE 420643, Systems Engineering, Department of Mechanical Engineering, Eindhoven University of Technology, Eindhoven, The Netherlands.

Park, S., J. W. Fowler, G. T. Mackulak, J. B. Keats, and W. M. Carlyle. 2002. "D-optimal Sequential Experiments for Generating a Simulation-based Cycle Time-Throughput curve". *Operations Research* 50 (6): 981–990.

Schoemig, A. K. 1999, December. "On the corrupting influence of variability in semiconductor manufacturing". In *Proceedings of the 1999 Winter Simulation Conference*, edited by P. A. Farrington, H. B. Nembhard, D. T. Sturrock, and G. Evans, 837–841. Piscataway, New Jersey: Institute of Electrical and Electronics Engineers, Inc.

Veeger, C., Y. Kerner, P. Etman, and I. Adan. 2011. "Conditional Inter-departure Times from the *M/G/s* Queue". *Queueing systems* 68 (3-4): 353–360.

Veeger, C. P. L., L. F. P. Etman, J. van Herk, and J. E. Rooda. 2010. "Generating Cycle Time-Throughput Curves using Effective Process Time based Aggregate Modeling". *IEEE Transactions on Semiconductor Manufacturing* 23 (4): 517–526.

AUTHOR BIOGRAPHIES

F.J.A. JANSEN Received his diploma in mechanical engineering from the Eindhoven University of Technology, April 2012. His master thesis study was on the topic presented in this paper. His email address is f.j.a.jansen@gmail.com.

L.F.P. ETMAN is an Associate Professor with the Manufacturing Networks group, Department of Mechanical Engineering, Eindhoven University of Technology, Eindhoven, The Netherlands. His current research interests include aggregate (simulation) modeling of queuing systems, simulation-based optimization, multi-disciplinary and systems design optimization. His email address is l.f.p.etman@tue.nl.

J.E. ROODA is Professor Emeritus, Department of Mechanical Engineering, Eindhoven University of Technology, Eindhoven, The Netherlands. His research interests include design and analysis of manufacturing systems, manufacturing control, and supervisory machine control. His email address is j.e.rooda@tue.nl.

I.J.B.F. ADAN is Full Professor of the Manufacturing Networks group, Department of Mechanical Engineering, Eindhoven University of Technology, Eindhoven, The Netherlands. His current research interests include the analysis of multi-dimensional Markov processes and queuing models, and the performance evaluation of communication, production, and warehousing systems. His email address is i.j.b.f.adan@tue.nl.